

# 1 Supplemental Material

## 2 Supplemental Methods

### 3 Cardiac <sup>31</sup>P-magnetic resonance spectroscopy

#### 4 *PCr/ATP*

5 Participants were positioned prone over a three-element dual-tuned <sup>1</sup>H/<sup>31</sup>P surface coil at magnet  
6 isocentre. An 11 min non-gated 3D acquisition-weighted ultra-short echo time CSI sequence was run  
7 as previously described<sup>21</sup>. Parameters included: acquisition matrix size 16 × 16 × 8 voxels, field of  
8 view 240 × 240 × 200 mm<sup>3</sup>, nominal voxel size 5.6 ml, 10 averages at the centre of k-space, fixed TR  
9 per-subject (910-1010 ms depending on specific absorption rate constraints), centre frequency 250  
10 Hz from PCr. The PCr/ATP ratio reported is the blood- and saturation-corrected PCr/average ATP  
11 ratio, averaged over the two most basal septal voxels. Spectral analysis was performed using  
12 “OXSA”, an open-source MATLAB implementation of the AMARES algorithm<sup>22</sup>.

#### 13 *CK k<sub>f</sub>*

14 CK k<sub>f</sub> was estimated using an implementation of triple repetition time saturation transfer (TRiST)  
15 modified to suit the 10 cm transmit-receive circular RF coil (PulseTeq Ltd, Chobham, UK) and  
16 multinuclear 3T scanner (Trio; Siemens, Erlangen, Germany) available at our centre<sup>23,24</sup>. With  
17 participants positioned supine for approx. 1 hour, we acquired transaxial and sagittal <sup>1</sup>H localisers to  
18 confirm coil position over the apical LV septum and at magnet isocentre (repositioning until satisfied),  
19 free induction decay (FID) inversion recovery scans of a phenylphosphonic acid (PPA) fiducial to  
20 calibrate transmit field (B<sub>1</sub><sup>+</sup>), imaging of cod-liver oil position markers (to calibrate coil position), and a  
21 transaxial slice level with the coil centre (for voxel placement). A 1D phase-encoded CSI matrix (16  
22 slices, 160 mm) was oriented coronally with sixteen 1 cm-deep voxels aligned parallel to the chest  
23 wall, aiming to place two voxels anterior to the chest surface and the voxel of interest (VOI) over the  
24 most apical unambiguously cardiac voxel.

25 A 5 min frequency-finding sequence (1D-CSI, 16 phase encode steps for depth selectivity, TR 330  
26 ms, TE 2.3 ms, flip-angle 35°, 125 averages, centre frequency 250 Hz negative to PCr) was run with a  
27 25 mm saturation band placed over chest wall skeletal muscle. This was analysed in MATLAB on a

28 computer adjacent to the scanner console to generate expected centre frequencies and frequency  
29 offsets of each of the 16 voxels. Those for the VOI were programmed for the four TRiST acquisitions.  
30 These comprised a fully-relaxed acquisition (TR 15 s, 2 averages, 9 min), two with selective  $\gamma$ ATP  
31 saturation (TR 1.5 then 9.5 s, 18 then 8 averages, 11 then 21 min), and one with control saturation  
32 mirrored around PCr (TR 15 s, 2 averages, 9 min), with pulse sequences and spectral analysis as  
33 described previously<sup>24</sup> generating a 1D coronal stack of  $k_f$  values. The value in the VOI was exported  
34 for group statistical analyses. To allow comparison with published literature  $k_f$  was adjusted for the  
35 effects of our supine coil position (vs prone in previous studies) by multiplying by 1.333 (as described  
36 previously)<sup>24</sup>.

### 37 Biochemical analysis of LV biopsies

38 10-20 min after going on cardiopulmonary bypass, surgical myocardial biopsies were obtained from  
39 LV endocardium and immediately divided into two parts. The larger part was frozen in liquid nitrogen  
40 within twenty seconds of excision and the smaller, a thin sample (roughly 0.5 × 1 mm), was bathed in  
41 primary fixative and further divided into parts three times smaller for electron microscopy. The larger  
42 part was stored at -80 °C until analysis. All biochemical analyses were performed on ice unless  
43 otherwise specified.

44 Samples were crushed into powder using a metal pulveriser precooled with dry ice. A heaped spatula-  
45 full of frozen, crushed powdered LV (5–10 mg) was reconstituted in a droplet of ice-cold  
46 homogenizing buffer ( $K_2HPO_4$  0.08 M,  $KH_2PO_4$  0.02 M,  $\beta$ -mercaptoethanol 1 mM, EGTA 1 mM, pH  
47 7.4), excess liquid chased off and the weight of tissue recorded. The sample was placed in a glass  
48 homogenising vessel with additional ice-cold homogenisation buffer, with the buffer volume adjusted  
49 to achieve a tissue concentration in buffer of 5 mg/ml. The sample was then homogenised using a  
50 stirrer at 1300 rpm for 30 sec. A 200  $\mu$ l aliquot of the homogenate was mixed with 200  $\mu$ l of 4% NaOH  
51 to create a solution for the Lowry assay. This solution was heated in a water bath at 60°C for two  
52 hours then stored at 4°C until analysis. The remainder was settled for 30 min at 4°C with 0.1% Triton-  
53 X 100 to permeabilize membranes. The resulting supernatant was used for subsequent  
54 measurements.

55 *CK activity*

56 Supernatant was diluted 1:5 in ice-cold homogenization buffer and kept on ice. CK-NAC reagent  
57 (catalogue code TR14010, Thermo Fisher Scientific) was warmed to 30°C in a water bath. At the point  
58 of measurement, 20 µl of diluted supernatant was placed in a cuvette and 1 ml CK-NAC was added.  
59 The rate of increase of absorbance of NADPH at 340 nm and 37°C, which is proportional to CK  
60 activity, was then monitored over 10 min using a spectrophotometer. CK velocity (IU/ml) was  
61 calculated from the rate of change in absorbance of NADPH, corrected for reaction volume and an  
62 assay-specific correction factor, averaged over three runs and normalised to Lowry protein (mg/ml).  
63 Results were presented as CK velocity (IU/mg protein).

64 *CK isoforms*

65 5 µl of supernatant was diluted 1:20 with ice-cold homogenization buffer and incubated with SPIFE  
66 CK vis activator (SAS-1+ kit, cat. no. 3332, 3333, Helena Biosciences) at room temperature for 10  
67 min. The mixed CK isoenzyme reagent underwent agarose gel electrophoresis using SAS-1+ kits to  
68 separate CK isoenzymes based on electrophoretic mobility. The separated isoenzyme bands were  
69 visualised by adding isoenzyme reagent and isoenzyme chromogen to the gel after 30 min. The gel  
70 was then incubated (60°C, 20 min), destained (0.3% acetic acid, 10 min), washed, dried (60°C, 30  
71 min) and scanned (ChemiDoc MP Imager, Bio-Rad). The relative concentration of bands was  
72 quantified by densitometry.

73 *Citrate synthase activity*

74 50 µl of supernatant was incubated with 850 µl of reagent (acetyl-CoA 0.35 mM, 5,5'-dithio-bis(2-  
75 nitrobenzoic acid) (DTNB) 0.12 mM; all solutions made up in Tris base adjusted to pH 8.1) for 3 min at  
76 room temperature. 100 µl of 10 mM oxaloacetate was added and absorbance at 412 nm monitored  
77 over 1 min. Mean activity over 40 s and two runs was reported in IU/mg protein.

78 *Total creatine concentration*

79 'Standards' containing known standard concentrations of creatinine, creatine, PCr, AMP, ADP and  
80 ATP were run through the HPLC column (Supelcosil™ LC-18-T, 5 µmol, cat. no. 58971, Sigma  
81 Supelco) at three dilution strengths and their concentrations plotted against peak area under the  
82 chromatogram to generate calibration curves for each molecule.

83 Frozen crushed LV was homogenised in perchloric acid, neutralised with potassium hydroxide,  
84 adjusted to pH 7, centrifuged at 4°C and filtered. All preparation was done on ice. 10 µl of  
85 homogenate was loaded onto the HPLC column under standard conditions (28°C, flow rate 0.7  
86 ml/min, detection wavelength 206 nm, mobile phase 3.5% acetonitrile, 215 mM potassium dihydrogen  
87 orthophosphate, 2.3 mM tetrabutylammonium bisulphate). Concentrations (nmol/ml) were normalised  
88 to Lowry protein (mg/ml) and presented as nmol/mg protein.

### 89 *Lowry protein concentration*

90 The solution for the Lowry assay was diluted in triplicate in water (1:10 for CK and CS assays, 1:50  
91 for creatine assays). Duplicate control 'standards' were made using known concentrations of BSA 0-  
92 80 µg/ml. Samples and standards were mixed with 1 ml Lowry reagent, vortexed and incubated at  
93 room temperature for 20 min. 500 µl Folin and Ciocalteu's phenol reagent was added and samples  
94 were vortexed and incubated at room temperature for 30 min. Samples were then filtered into  
95 cuvettes (3 ml syringe, 0.45 µm filter) and protein concentration quantified by measuring absorbance  
96 at 750 nm.

### 97 Serial block-face scanning electron microscopy (SBF-SEM)

#### 98 *Sample fixation and imaging*

99 The purpose of the SBF-SEM was to generate 3D sarcomere-mitochondrion distance maps for each  
100 dataset, which would represent diffusion distance distributions for high-energy phosphates. This  
101 influenced the choices and compromises made below, in particular: resolution was not optimised for  
102 assessment of mitochondrial number or health; alternate slices were analysed rather than single  
103 slices to maximise 3D coverage.

104 Newly separated biopsies were transferred to freshly prepared primary fixative (2.5% glutaraldehyde  
105 + 4% formaldehyde in 0.1M sodium cacodylate buffer, pH 7.4) as soon as possible then stored at 4°C  
106 for up to four weeks before batch processing. Samples were then washed and underwent secondary  
107 fixation A with osmium ferricyanide (1.5% potassium ferricyanide + 2% osmium tetroxide in 0.1M  
108 sodium cacodylate buffer). Samples then underwent further washing and staining cycles with  
109 thiocarbohydrazide, 2% osmium tetroxide (secondary fixation B), 1% uranyl acetate (overnight tertiary  
110 fixation), and lead aspartate, followed by dehydration cycles with increasing concentrations of

111 anhydrous ethanol (30–100%) and 100% acetone (day 2). After dehydration, samples were infiltrated  
112 with Durcupan epoxy resin (with acetone as the transition solvent) overnight and incubated in a  
113 microwave processing unit (Leica AMW), then embedded in flat bottom Beem capsules in fresh  
114 Durcupan resin and polymerised at 60 °C for 72 hrs.

115 Acquisition parameters were determined by experimentation, aiming to achieve sufficient resolution to  
116 identify mitochondrial outlines but balancing this against achieving a wide field of view and acceptably  
117 short time per slice. Pressure was tuned to reduce charging of the sample surface. Typical acquisition  
118 parameters (magnification 6100x, voltage 3 kV, dwell time 6 ms, pressure 0.3 Torr, field of view 40  
119  $\mu\text{m}$  square or 4000  $\times$  4000 pixels, slice thickness 100 nm, pixel pitch 10  $\times$  10 nm) resulted in  
120 approximately 220 slices serially sectioned and imaged over 24 hours for each dataset.<sup>46-48</sup>

### 121 *Sample analysis*

122 Manual segmentation was performed over 30 alternate slices to improve the existing model, aiming to  
123 define areas as mitochondria, sarcomere or neither. Due to the time-intensive nature of the task and  
124 the redundancy within the data (the typical z-dimension of a mitochondrion spanned ~5-6 consecutive  
125 slices), alternate- and consecutive-slice segmentation strategies were compared for one dataset. As  
126 the results were similar, an alternate-slice approach was taken. Each dataset required 7-21 working  
127 days to manually segment to a satisfactory standard.<sup>46-47</sup>

128 After manual segmentation, the shortest distance for any pixel labelled sarcomere to the nearest pixel  
129 labelled mitochondrion in 3D, here called diffusion distance, was computed across the 3D dataset  
130 using a MATLAB script supplied by Dr Ilya Belevich. Raw histograms of the diffusion distances  
131 displayed modal spikes at multiples of the inter-slice z distance, reflecting an artefact of the voxel  
132 dimension ratio (1:1:10). To mitigate this, a linear interpolation script (MATLAB's "interpmask") was  
133 run on both the stack of 8-bit tiffs and the manually segmented model, such that four synthetic slices  
134 were interpolated between each pair of consecutive slices (5-fold interpolation for tiffs). Similarly, 10-  
135 fold interpolation was run on the model in the z-direction and 0.5-fold interpolation in the xy plane,  
136 resulting in isotropic 20 nm voxels and so reducing the matrix size from 4000  $\times$  4000  $\times$  4000 to 2000  $\times$   
137 2000  $\times$  301. Diffusion distance distributions were thus smoothed. While resembling log-normal  
138 distributions, no single parameter could perfectly summarise the distributions, and median distance  
139 was reported.

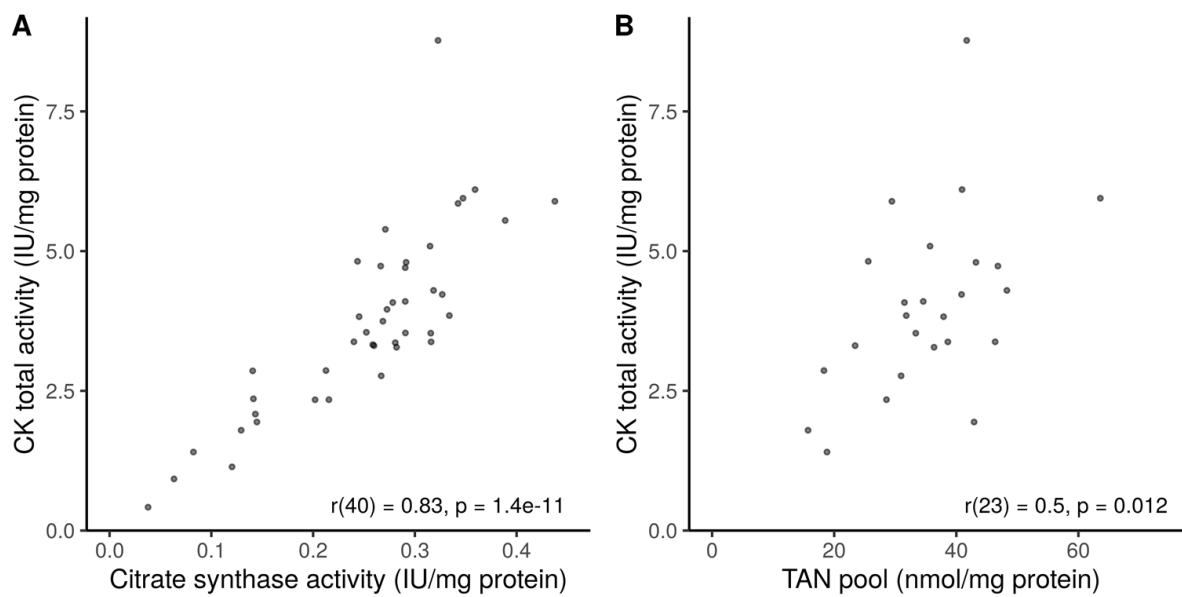
140 Supplemental Tables

141 Supplemental Table I. Invasive and non-invasive correlates of CK total activity.

Parameter	N	Pearson r	p-value (r)	Spearman rho	p-value (rho)
CS total activity (IU/mg protein)	42	.83	$1 \times 10^{-11}$	.83	$2 \times 10^{-16}$
CK/CS activity ratio (IU/IU)	42	.61	$2 \times 10^{-5}$	.52	$5 \times 10^{-4}$
TAN pool (nmol/mg protein)	25	.50	.012	.50	.012
Total creatine (nmol/mg protein)	42	.57	$9 \times 10^{-5}$	.58	$8 \times 10^{-5}$
CK $k_f$ adj (/s)	32	.45	.009	.33	.070
$k_f$ adj $\times$ estimated [PCr] ( $\mu$ mol/g/s)	30	.37	.044	.38	.041
$k_f$ adj $\times$ total creatine (nmol/mg/s)	32	.65	$5 \times 10^{-5}$	.58	$7 \times 10^{-4}$
LVEDVi (ml/m <sup>2</sup> )	41	-.51	$6 \times 10^{-4}$	-.55	$3 \times 10^{-4}$
LVESVi (ml/m <sup>2</sup> )	41	-.50	$9 \times 10^{-4}$	-.44	.005
LVEF (%)	41	.40	.011	.30	.053
LVMi (g)	41	-.44	.004	-.47	.002
MRI global circumferential strain (%)	39	-.52	$7 \times 10^{-4}$	-.45	.004

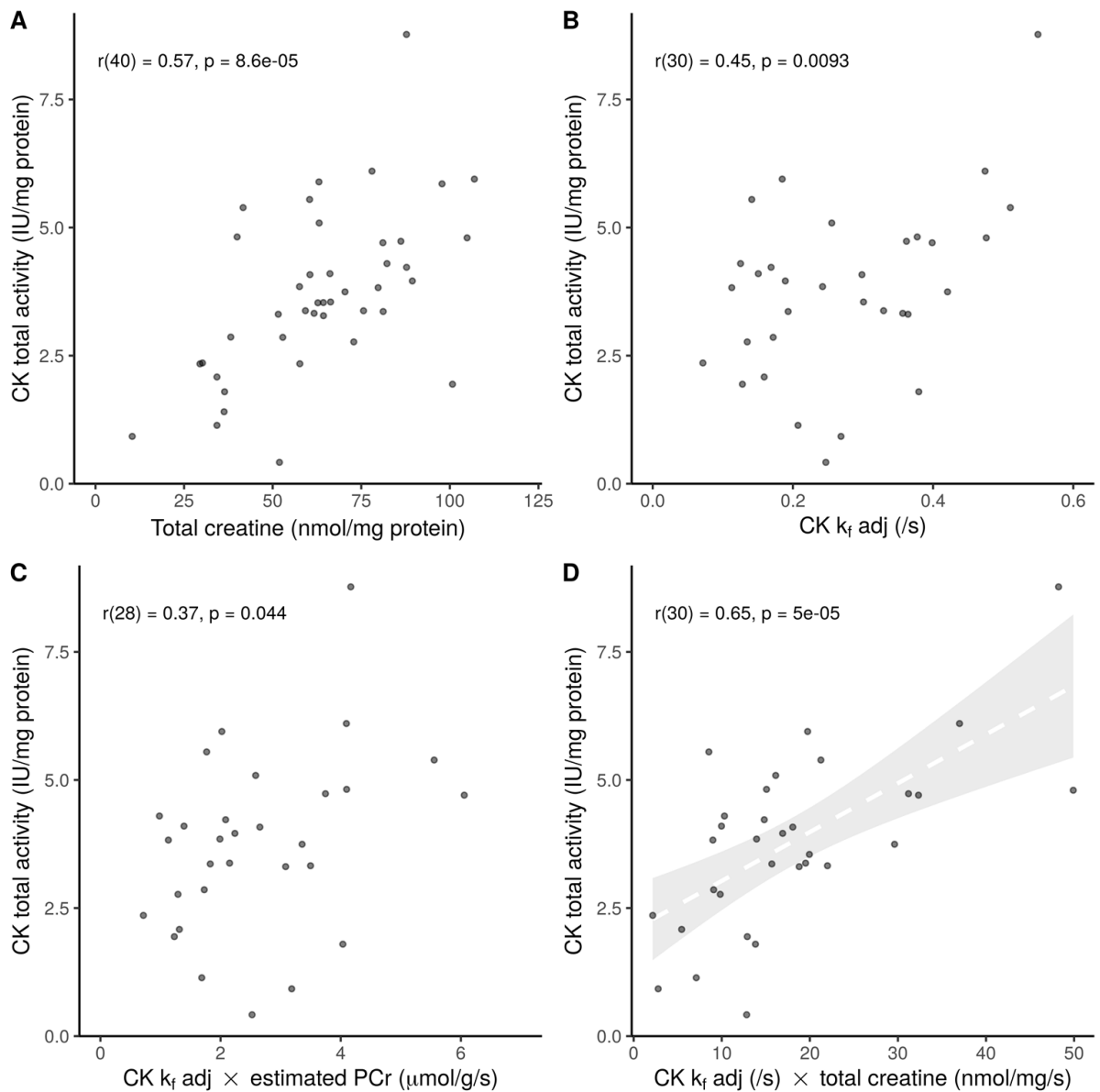
142

143 Supplemental Figures



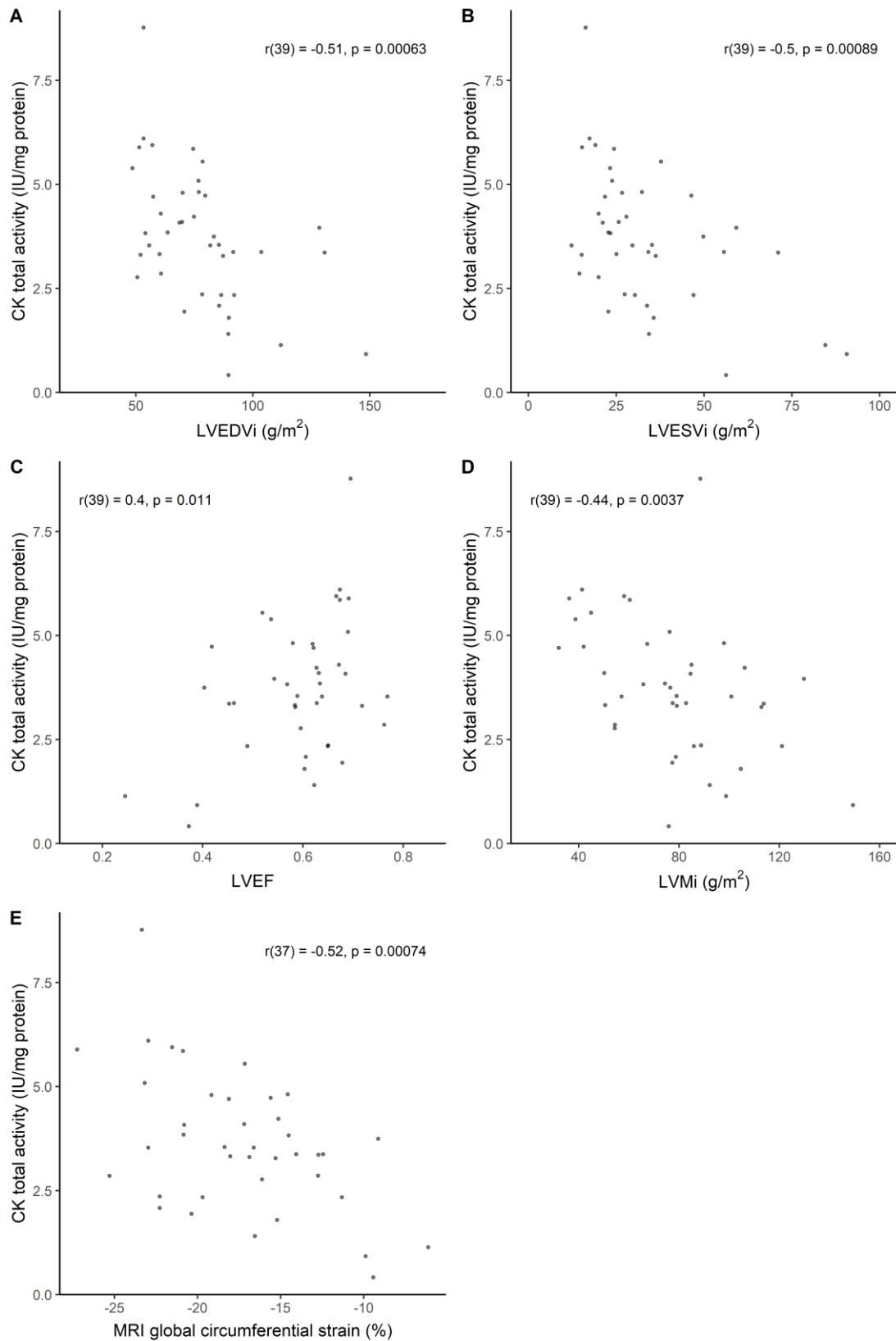
144 **Supplemental Figure I.** Scatter plots for (A) citrate synthase (CS) activity, (B) total adenine

145 nucleotide (TAN) pool against CK total activity.



146 **Supplemental Figure II.** Scatter plots for (A) total creatine, (B) CK  $k_f$  (adjusted for supine position),  
 147 (C) CK flux estimated by  $k_f \times$  estimated [PCr], and (D) CK flux estimated by total creatine  $\times k_f$  against  
 148 CK total activity.





149

150 **Supplemental Figure III.** Scatter plots for (A) left ventricular end-diastolic volume index, (B) left  
 151 ventricular end-systolic volume index, (C) left ventricular ejection fraction, (D) left ventricular mass  
 152 index, and (E) MRI global circumferential strain against CK total activity.



